



저작자표시-비영리-변경금지 2.0 대한민국

이용자는 아래의 조건을 따르는 경우에 한하여 자유롭게

- 이 저작물을 복제, 배포, 전송, 전시, 공연 및 방송할 수 있습니다.

다음과 같은 조건을 따라야 합니다:



저작자표시. 귀하는 원저작자를 표시하여야 합니다.



비영리. 귀하는 이 저작물을 영리 목적으로 이용할 수 없습니다.



변경금지. 귀하는 이 저작물을 개작, 변형 또는 가공할 수 없습니다.

- 귀하는, 이 저작물의 재이용이나 배포의 경우, 이 저작물에 적용된 이용허락조건을 명확하게 나타내어야 합니다.
- 저작권자로부터 별도의 허가를 받으면 이러한 조건들은 적용되지 않습니다.

저작권법에 따른 이용자의 권리는 위의 내용에 의하여 영향을 받지 않습니다.

이것은 [이용허락규약\(Legal Code\)](#)을 이해하기 쉽게 요약한 것입니다.

[Disclaimer](#)

Master's Thesis  
석사학위 논문

**Development of a Real-Time Multimodal 3D Endoscope  
for Detection of Various Gastric Lesions**

Sehyo Youn(윤 세 효 尹 世 孝)

Department of the Information and Communication

정보통신융합공학 전공

**DGIST**

**2016**

Master's Thesis  
석사 학위논문

**Development of a Real-Time Multimodal 3D Endoscope  
for Detection of Various Gastric Lesions**

Sehyo Youn(윤 세 효 尹 世 孝)

Department of the Information and Communication

정보통신융합공학 전공

**DGIST**

**2016**

**Development of a Real-Time Multimodal 3D Endoscope  
for Detection of Various Gastric Lesions**

Advisor : Professor Jaeyoun Hwang

Co-advisor : Professor Cheol Song

by

Sehyo Youn

Department of the Information and Communication  
DGIST

A thesis submitted to the faculty of DGIST in partial fulfillment of the requirements for the degree of Master of Science in the Department of the Information and Communication. The study was conducted in accordance with Code of Research Ethics<sup>1</sup>

1. 8 .2016

Approved by

Professor Hwang Jae Youn ( Signature )  
(Advisor)

Professor Song Cheol ( Signature )  
(Co-Advisor)

---

<sup>1</sup> Declaration of Ethical Conduct in Research: I, as a graduate student of DGIST, hereby declare that I have not committed any acts that may damage the credibility of my research. These include, but are not limited to: falsification, thesis written by someone else, and distortion of research findings or plagiarism. I affirm that my thesis contains honest conclusions based on my own careful research under the guidance of my thesis advisor.

**Development of a Real-Time Multimodal 3D Endoscope  
for Detection of Various Gastric Lesions**

Sehyo Youn

Accepted in partial fulfillment of the requirements for the degree of Master of  
Science

12. 3 .2015

Head of Committee Jae Youn Hwang (인)

Prof. 황재윤

Committee Member Cheol Song (인)

Prof. 송철

Committee Member Kijoon Lee (인)

Prof. 이기준

Degree  
201422011

윤 세 호. Sehyo Youn. Development of a Real-Time Multimodal 3D Endoscope for Detection of Various Gastric Lesions. Department of the Information and Communication. 2016. 69p. Advisor Prof. Hwang, Jae Youn, Prof. Co-Advisor Song, Cheol.

### ABSTRACT

We built a multimodal endoscopic imaging system capable of fluorescence intensity, reflectance/fluorescence multi-spectral, and real-time 3-dimensional (3D) stereoscopic imaging for detection of gastric lesions. The system consists of two fiber bundles where GRIN Lens are attached to the end of them for collection of light from a region of interest, an objective lens for relaying of the collected light into a high sensitive CCD camera, optical bandpass filters included in a filter wheel, a servo-motor for selection of the bandpass filter, a beamsplitter, and etc. Also, a system control program was developed in order to perform fluorescence, multispectral, and 3-D stereoscopic imaging. Moreover, an ultrasound biomicroscopic system was developed for acquisition of a B-mode ultrasound image of a gastric lesion. It will be incorporated with the multimodal endoscopic system we developed. The capability of each imaging modality was here evaluated with tissue phantoms and then it was applied to image GI tumors *ex-vivo* in order to investigate its potential to discriminate between tumors and normal regions. The images obtained using each imaging modality showed that the tumor regions were clearly distinguished from the normal regions. Altogether, our developed system here allowed to obtain different but complementary information on lesions of interest such as auto-fluorescence intensity, spectral signatures, 3D surface curvatures and invasion depth of the lesions, thus may enhance the contrast in the early detection of gastric lesions.

Keywords: Multimodal imaging, auto-fluorescence, multispectral, 3D imaging, high frequency ultrasound imaging, cancer detection

# Contents

Abstract .....	i
I . INTRODUCTION .....	1
II. METHOD	
2.1 Configuration of the total system .....	5
2.2 Connection between Optical fiber bundle and GRIN Lens .....	6
2.3 Multi-spectral reflectance imaging system .....	7
2.4 Fluorescence intensity imaging system .....	8
2.5 Multi-spectral fluorescence intensity imaging system .....	8
2.6 3-Dimensional stereoscopic imaging system .....	8
2.7 Software .....	10
2.8 Circuit .....	11
2.9 Ultrasound Biomicroscopy .....	12
III. PHANTOM EXPERIMENT	
3.1 Make a phantom .....	14
3.2 Reflectance imaging .....	14
3.3 Fluorescence and fluorescence spectral imaging .....	15
3.4 Ultrasound Biomicroscopy imaging .....	16
3.5 3-Dimensional stereoscopic imaging .....	16
3.6 GPU speed experiment .....	17
IV. TUMOR <i>ex vivo</i> EXPERIMENT .....	18
V . DISCUSSION and CONCLUSIONS .....	20
VI. REFERENCE .....	21
VII. APPENDIX .....	26

## I . INTRODUCTION

Globally, one-third of adult people suffer from cancer. Among the cancer, the incidence rate of colorectal and gastric cancer is above 60%. In the case of colorectal cancer, early detection and removal of colorectal adenomatous polyps is crucial for increasing the survival rate of patients with colorectal cancer. To date, various types of endoscopic imaging systems have been developed for diagnosis of gastric or colorectal neoplasm. However, the detection and localization of early gastric or colorectal neoplasm *in vivo* with high specificity and sensitivity still remain very challenging by using the existing endoscopic systems. Therefore, many researchers have so far developed a variety of more advanced endoscopic imaging systems with combination of different imaging modalities.

There are various imaging modalities available for medical and biological applications, including fluorescence, multispectral, 3-D, and ultrasound imaging. Among them, multispectral imaging has been considered as one of the most quantitative imaging methods in optical imaging techniques, capturing image data at specific frequencies across the electromagnetic spectrum. The wavelengths may be separated by filters or by the use of instruments that are sensitive to particular wavelengths, including light from frequencies beyond the visible light range, such as infrared. Spectral imaging can allow extraction of additional information the human eye fails to capture with its receptors for red, green and blue. It was originally developed for space-based imaging. White light have been used commonly in endoscopic systems. However, early gastric or colorectal cancer is not seen with the naked eye using white light source. Therefore, multi-spectral imaging, which can analyze each of the wavelength of the reflectance light from early cancer and normal tissue, has been utilized for better detection of the cancer. Multi-spectral reflectance imaging allowed to discriminate between cancer-

ous lesion and normal lesion in ex-vivo experiment [2], [3]. Therefore, it has been utilized as a very promising tool in detection of various lesions [6], [37].

Fluorescence imaging is an ideal technique for examining fixed and living specimen. Using the phenomenon that certain materials emit energy detectable as visible light when excitation of the materials with light at a specific wavelength, fluorescence imaging allows detection of the changes in target molecule concentrations with a good signal-to-noise ratio. Human tissues emit their inherent fluorescence called autofluorescence when they are illuminated by light at a specific wavelength. Using this property, autofluorescence endoscopy was utilized to detect early carcinomas and discriminate between normal tissue and neoplastic lesions [4], [36].

3-D stereoscopic imaging has also been utilized in medicine and biology. In 3-D stereoscopic imaging, the illusion of depth in an image is created and enhanced by means of stereopsis for binocular vision. The stereoscopic image is here called a stereogram. Originally, stereogram referred to a pair of stereo images which could be viewed using a stereoscope. Most stereoscopic methods offer two offset images separately to the left and right eye of the viewer. These two-dimensional images are then combined in the brain to give the perception of 3D depth. This technique is distinguished from 3D displays, allowing the observer to increase information about the 3-dimensional objects being displayed by head and eye movements. The stereoscopic method is a basic technique for three-dimension reconstruction of surface [5]. Most of the colorectal cancer are occurred from polyps. Also, gastric lesions such as tumors exhibit protrude or retracted regions. Through the 3D stereoscopic imaging, colorectal adenomatous polyps or gastric lesions can be detected by quantification of the roughness of the walls of the colon or gastric region.

Lastly, ultrasound biomicroscopy is a high resolution imaging technique which can be used in various fields

of medicine and biology, primarily for detection, follow-up, and diagnosis of diseases and injuries in humans and animals. It provides tomography information without the needs for biopsy and longitudinal anatomical information *in vivo*. The ultrasound biomicroscopy frequencies used in most applications vary from 40 to 60MHz, corresponding to a resolution on the order of micrometer. Typically, frequencies range from 40 to 40MHz allows high resolved ultrasound images compared to the conventional ultrasound frequency for medical imaging [24] [38]. Especially, high frequency ultrasound systems have been used *ex vivo* to study intact and maturing cartilage, osteoarthritic cartilage and repair cartilage. Ultrasound quantitative measurements have also been developed to assess cartilage properties [51].

A multi-modal endoscope system have been developed for detection of various diseases. In L. Marcu group, they presented a multimodal endoscopic system which includes florescence lifetime imaging and autofluorescence imaging, for *in vivo* intraoperative diagnosis of oral carcinoma [34]. Also, Lihong V. Wang and K. Kirk Shung presented the endoscope system which combining photoacoustic and ultrasound imaging for examination of internal organs *in vivo* [35]. Since these the systems have several limitations such as allowing few molecular and anatomical information, may reduce the specificity and sensitive in the detection of cancerous regions, and also offering limited capability for obtaining a growth level or invasion depth of the cancer and 3-D surface information. Therefore, development of a multimodal endoscope system, capable of offering cancer invasion depth, surface roughness, and various molecular information on early gastric or colorectal cancerous lesions, simultaneously, would offer better sensitivity and selectivity in the detection of gastric and colorectal lesions.

In this paper, we thus built a novel multimodal endoscopic imaging system capable of fluorescence intensity, reflectance/fluorescence multispectral, and real-time 3D imaging via General Purpose Graphics Pro-

cessing Units (GPGPU) processing. An ultrasound microscopic system has also been developed for acquisition of tumor invasion into a target tissue. It will be incorporated with the endoscope. Each imaging modality was here evaluated with tissue-mimicking phantoms and then applied to detect early colorectal cancer *ex vivo*, thus demonstrating its potential to detect gastric lesions with high quantitate and specificity.

## II. METHOD

### 2.1 Configuration of the system

The multimodal endoscopic system developed is represented figure 3. The system consist of the GRIN Lens (Imaging Focusing Rod Lens, diameter=1.0mm, working distance=10mm, lens length=2.54mm, NA=0.5, non-coated, GT-IFRL-100-020-50-NC, GRINTECH), which do not have the aberrations typical of traditional spherical lenses, CCD(PIXIS 400) which is sensitive sensor for fluorescence imaging, two fiber bundles(Fujikura, FIGH-40-920G L=1,500 mm,  $\phi$  =1mm, pixel:40,000) for stereoscopic imaging, optical bandpass filter(band width=10nm, 500-680nm, Edmundoptics) for multi-spectral imaging, beamsplitter(50:50, THORLABS), High Power white light lamp(HPLS-30-03, THORLABS), high power UV lamp(CS2010, 365nm, THORLABS), servo-motor(DYNAMIXEL XL-320, ROBOTIS), Objective lens(10x, OLYMPUS), filter wheel, which is printed 3D printer and Micro Controller Unit(ATmega128, Atmel), and some optical components.

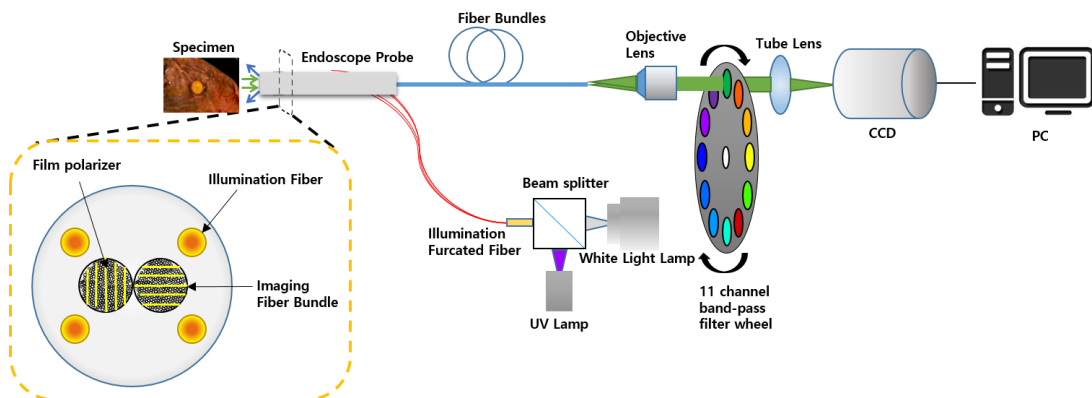
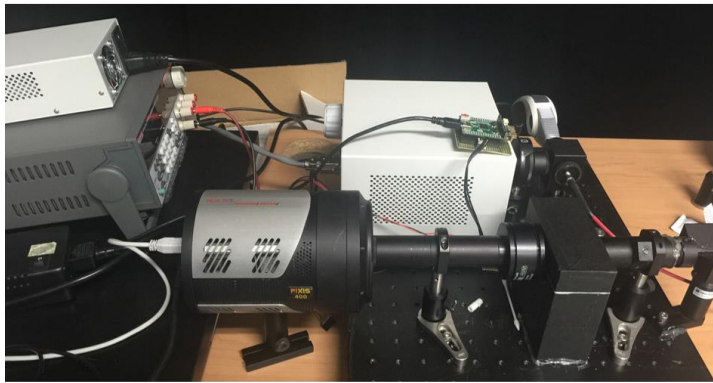
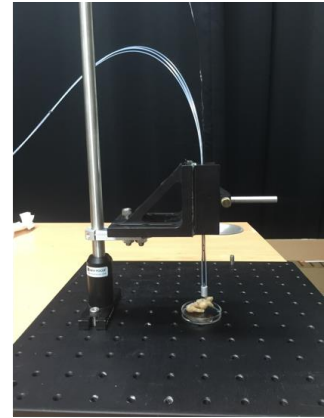


Figure 1. A schematic diagram of the multimodal endoscope system.



(a)



(b)

**Figure 2. (a) is constructed endoscope imaging system. (b) represents the detection part of the system.**

## 2.2 Connection between Optical fiber bundle and GRIN Lens

In order to obtain clearly image, connection between optical fiber bundle and GRIN Lens is very important. If there are some alien substances or air gab, obtained image quality is deteriorated. Because, the light is very sensitive about difference of a refractive index. So, when we connected between optical fiber bundle and GRIN Lens, we used shrinkable tube, UV epoxy, and high power UV light. Due to the shrinkable tube is flexible, then applying heat to shrink beforehand. Then, insert the optical fiber bundle and GRIN lens at both ends of shrinkable tube. And, put the UV epoxy at the connection point. Using high power UV light, illuminate in other parts of the epoxy about three minute. Figure 4 represent about above process.

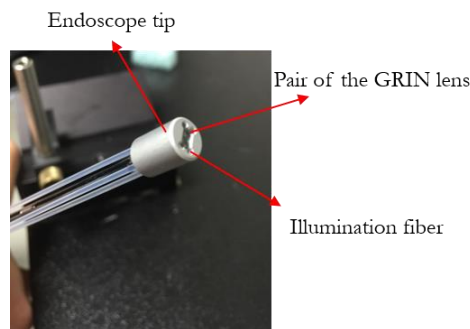


**Figure 3. It is an endoscope tip which is combined pair of the GRIN Lens and Illumination fibers.**

### 2.3 Multi-spectral reflectance imaging system

Using filter wheel which is made by using 3d printer, optical band pass filters (500nm-680nm) are located each hole in the filter wheel. The white light from white light led is illuminate the gastric lesion through the optical fiber ( $\phi=0.7\text{mm}$ ). For reflectance spectral imaging, the light from a mercury lamp was delivered to a specimen after passing through a furcated multimode fiber. The reflected light from the specimen was collected by GRIN lenses attached to two optical fiber bundles. Sequential wavelength selection from 500 nm to 680 nm was then realized by bandpass filters installed in a motorized filter wheel and then recorded in CCD to create a 3D image cube. In the spectral classified image (figure 5), the green-color represents sample area while the red-color represents shadow regions.

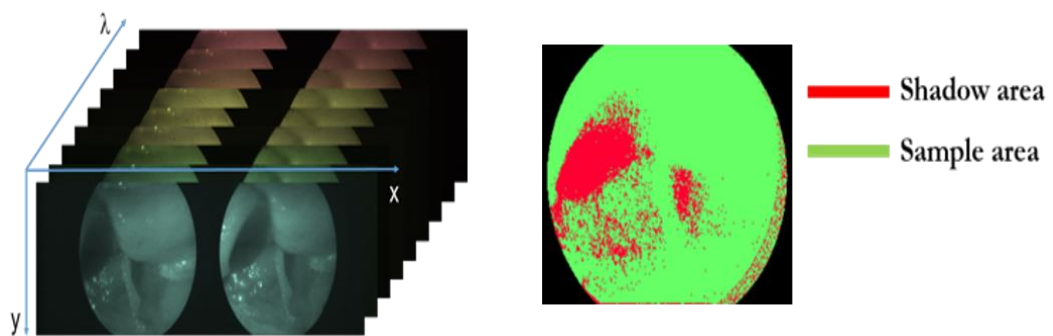


**Figure 4. Obtained image cube and classification result from the phantom.**

### 2.4 Fluorescence intensity imaging system

For fluorescence imaging, the light emitted from gastric lesions excited by light at 480 nm was selected with a bandpass filter at 530 nm and recorded in a charge-coupled device (CCD). The strong fluorescent regions in the image (figure 6) indicate fluorescent dyes.

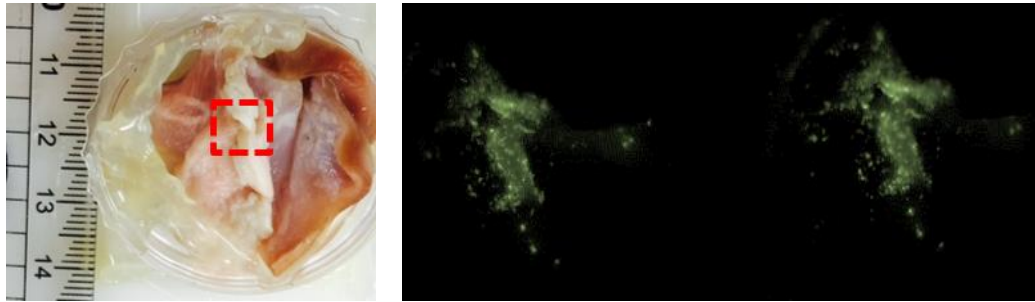


**Figure 5.** Left one represents about phantom which is stained by using fluorescence bead. Right one represents about fluorescen image from the phantom. Excitation light is 480nm and emission light is 530nm.

### 2.5 Multi-spectral Fluorescence intensity imaging system

For fluorescence multispectral imaging, light at 480 nm was applied to gastric lesions of interest for excitation. The wavelength of the emitted light was sequentially selected with the aforementioned manner, followed by spectral classification.

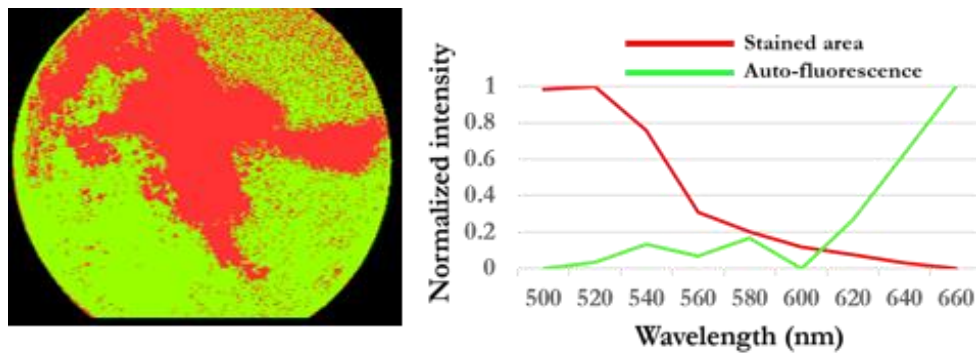


**Figure 6.** The result of classification from multi-spectral fluorescence image cube and spectral signature.

### 2.6 3-Dimensional Stereoscopic imaging system

Two optical fiber bundles are utilized for real-time 3-D stereoscopic imaging. The 3-D image provided 3-D surface curvatures of the sample. The process of 3D reconstruction is represented at figure 9. Sum of Absolute Differences (SAD) matching method (1) is applied for 3D reconstruction (figure 10). However, when

we applied generally SAD matching method, there are many noise as the figure 10. So, in order to improve image quality, we applied threshold method using applied window size (2).

$$disparity = \sum_{i=0}^{row} \sum_{j=0}^{col} |f(i + d, j) - f(i, j)| \quad (1)$$

$$Threshold = C * window\ size^2 \quad (2)$$

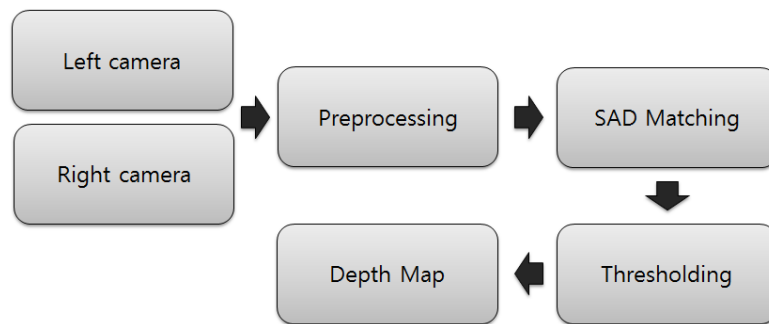


**Figure 7. Block diagram of 3D reconstruction using stereo image, SAM Matching method, and Thresholding method.**

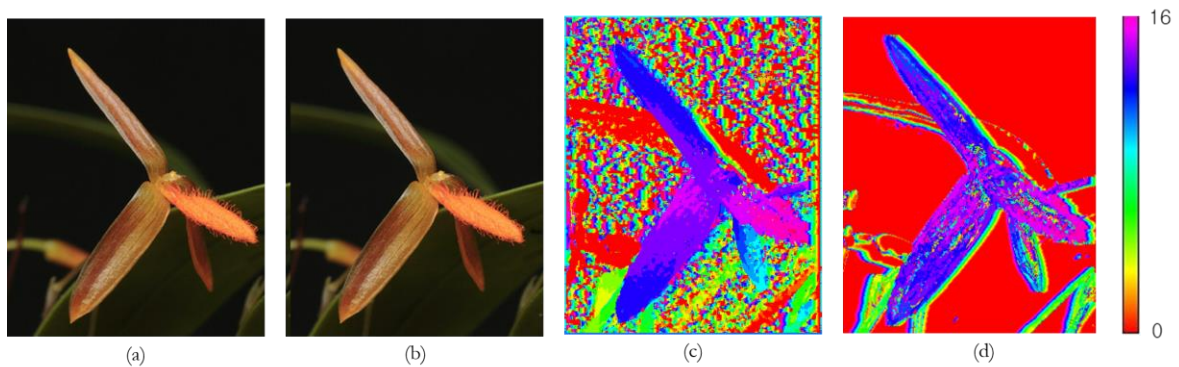


**Figure 8. (a),(b) stereo image (left and right) of plant. (c) result of the SAD matching method for (a) and (b). (d) result of Threshold method from (c).**

And, we applied second derivative for quantification of surface roughness from the depth map.

Through the second derivative we can count the number curvature of the surface changes. On the graph of a function, the second derivative corresponds to the curvature or concavity of the graph. The graph of a function with positive second derivative curves upwards, while the graph of a function with negative second derivative curves downwards. If the value of the roughness in the formula (3) is large, the image shows that much tough.

$$\text{Roughness} = \frac{\text{avg}\left(\sum_i^{\text{height}} \left| \frac{d^2 x_i}{dx^2} \right| \right)}{D_{\text{range}}} \quad (3)$$

## 2.7 Software

We implemented window program based on MFC (Microsoft Foundation Class). This program is involved serial communication with Micro controller unit (ATmega128), motor control, CCD sensor control, acquisition image data from each of imaging mode, and classification from obtained image data. Each imaging techniques are operated through the button operation, and obtains the image data.

In a figure 11, the display an image from the upper left corner of the window to be recorded through the CCD. By adjusting the exposure time, it may control the amount of light that is written to the CCD. When we click the start button, obtained image of the object is display, and the operation of the CCD is stopped by the stop button. In order to the above operations, stop button is operated by a different thread than the main thread. Because, if it is a continuous shooting because it is running an endless loop through the “while” syntax conversely it needs a thread to operate separately. In order to operate each of the imaging system, it needs filter wheel control through communication between ATmega128 and window program. Serial port number (ex.COM4) and communication speed are corresponded for prefer operation. In this system, we set COM4 which is serial port number and 115200bps which is communication speed. For convenience of the user, we made setting menu on the bottom of the program. And, for checking the communication with ATmega128, we made Text Box, which shows protocol.



**Figure 9. Implemented software for each of imaging systems**

In order to implement the real-time image processing, we applied parallel computing method based on General purpose Graphic Processing Unit (GPGPU) using CUDA from NVIDIA. CUDA is a parallel computing platform and programming model invented by NVIDIA. It enables dramatic increases in computing performance by harnessing the power of the graphics processing unit (GPU). With millions of CUDA-enabled GPUs sold to date, software developers, scientists and researchers are finding broad-ranging uses for GPU computing with CUDA.

## 2.8 Circuit

In order to control the motor for operating filter wheel, we made MCU board using ATmega128 and TTL chip which is buffer unit (74HC126). An operation receiving power from the PC through the USB cable, and the motor is supplied with power from an external power source.

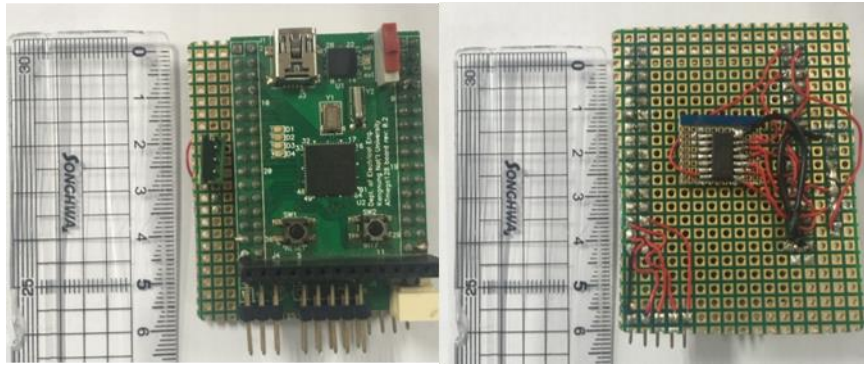


Figure 10. ATmega128 board and soldered buffer chip 74HC126.

## 2.9 Ultrasound Biomicroscopy

For ultrasound biomicroscopy, we made a phantom using pure water 133ml, agar powder 2.67g, and graphite 0.5mm. Mix the pure water and the agar powder and heat the mixture and then cool with the graphite.

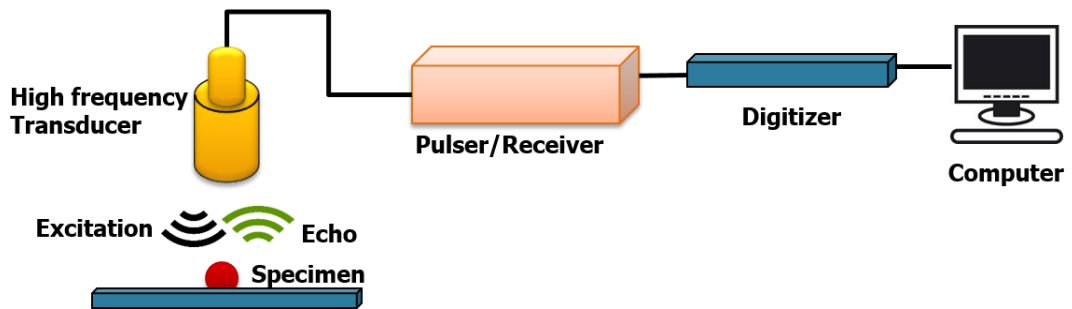
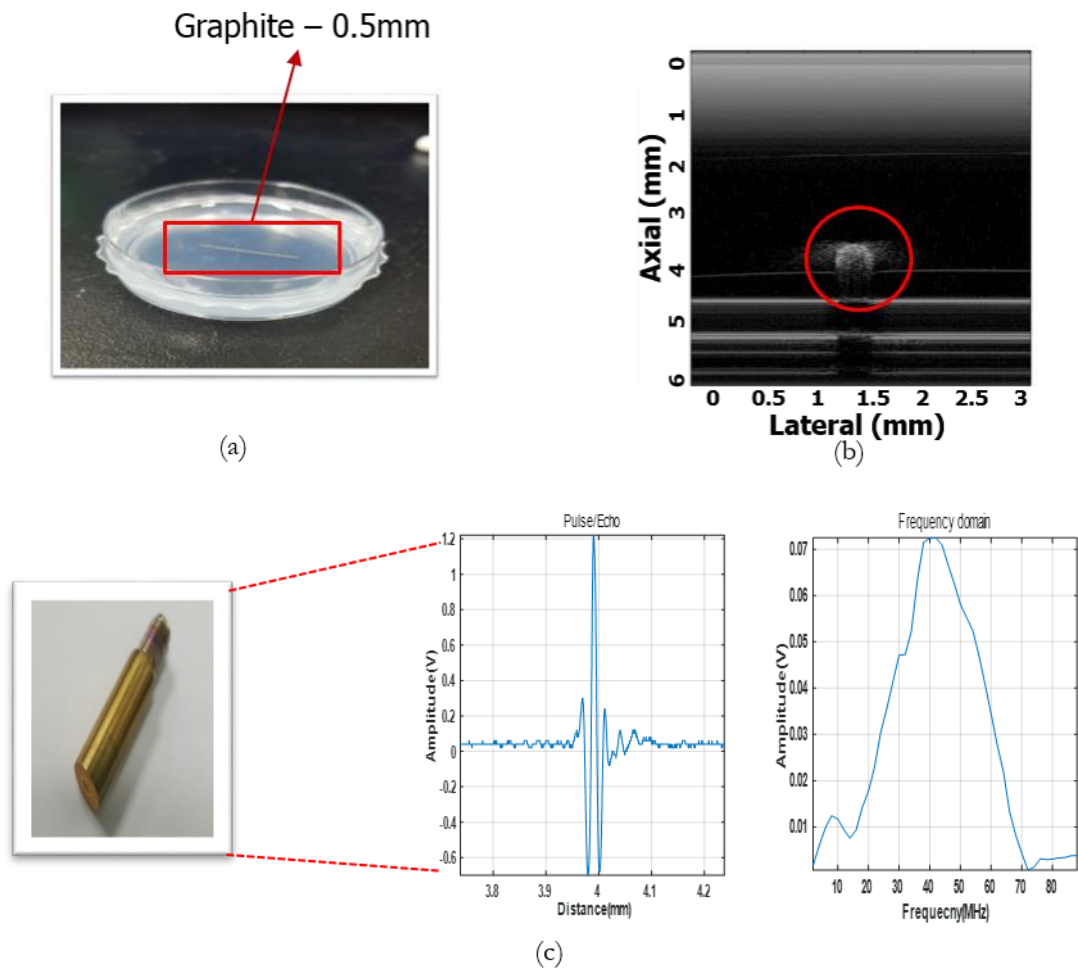


Figure 11. A schematic diagram of the ultrasound biomicroscopy system.



Figure 12. Siquence of the ultrasound image reconstruction.



**Figure 13. (a) Phantom is made by using pure water, agar power, and graphite. (b) Reconstructed ultrasound microscopy image from (a). (c) Results of pulse-echo test and frequency response of the used transducer.**

The ultrasound echo signal from Ultrasound Biomicroscopy system (figure 11) is reconstructed to image through the sequence (figure 12). The result of reconstruction represents figure 13(b). In the reconstructed image, we can find the graphite in the 4mm depth. It is the same result of pulse-echo specification of the used ultrasound transducer (left image of figure 13(c)) is the center figure of figure 13(c).

### III. PHANTOM EXPERIMENT

#### 3.1 Make a Phantom using a stomach of pig

In order to make a phantom, firstly we stained wood stick with fluorescent dye. And then, insert the stained wood in the piece of stomach of pig figure 14(c). To expressd gastric cancer in the gastric lesion, we didn't just stain surface of the specimen. We insert the actual dyed an object which is stained by fluorecence beads. When a phantom made, as shown in figure 14 it can be seen protruding compared to the surroundings.

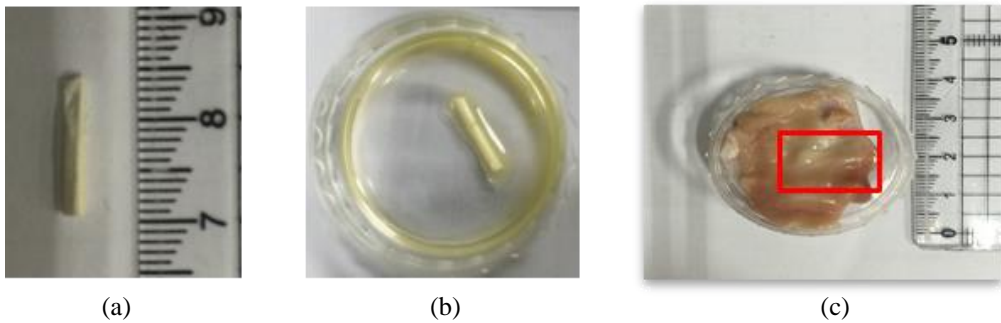


**Figure 14. (b) Wood stick stained with fluorescent dye. (c) A piece of stomach which is inserted stained wood stick in the red box.**

#### 3.2 Reflectance imaging

We experimented using above phantom and implemented software. Reflectance light through the two fiber bundles from the red box part of the figure14 is recorded in the CCD. Figure 15 represents about recorded image. As shown in the image, the object as shown in eyes can be ensured that the left and right imaging.

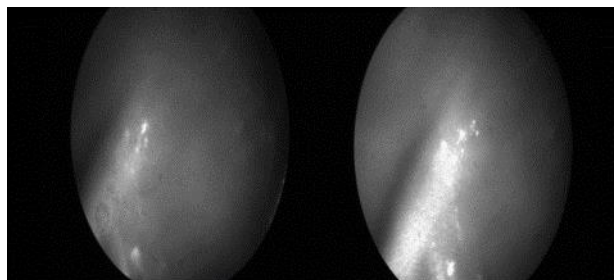


**Figure 15. The displayed image which is stored in the CCD reflected light from the phantom.**

### 3.3 Fluorescence intensity and fluorescence spectral imaging

In order to experiment the fluorescence imaging, firstly we determined the spectrum signature which is used to stain to phantom. And then, filtered light (480nm) from high power light source is illuminated to phantom. Figure 16(a) indicates that the emitted light from phantom is recorded in the CCD. And, figure 16(c) shows the spectrum of extracted from classification of fluorescence image cube. Red line represent fluorescence and green line represent auto-fluorescence from phantom.

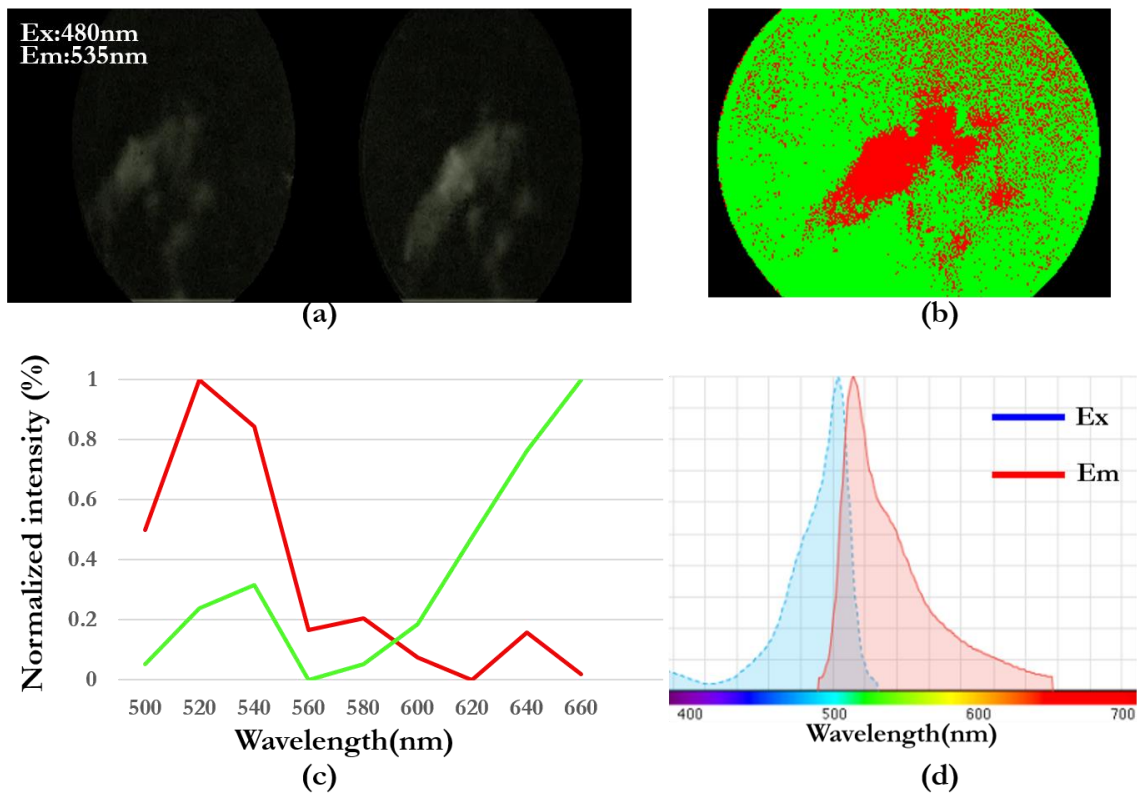
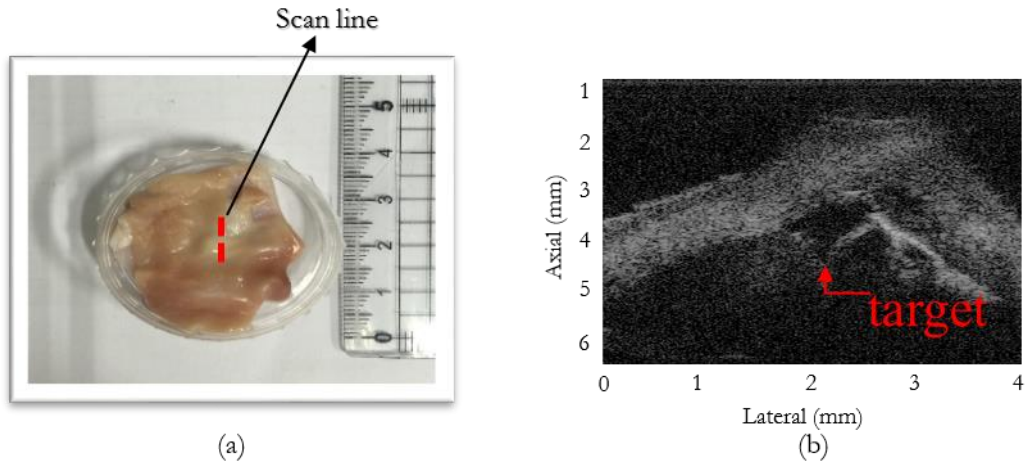


Figure 16. (a) Fluorescence imaging result. Excitation light is 475nm, emission light is 535nm. (b) The result of classification from fluorescence multi-spectral image cube. Red area represent fluorescence and green area represent auto-fluorescence from phantom. (d) Reference spectral signature of fluorescence bead which is used to make phantom. Blue one represent excitation light, red one represent emission light.

### 3.4 Ultrasound Biomicroscopy imaging

We performed ultrasound biomicroscopy imaging using phantom (figure 17 (a)) and the UBM system. As shown figure 17 (b), scan area is 4mm on lateral direction and 6mm on axial direction. And, wood stick in the phantom is detected in the 4mm depth and black area.



**Figure 17. (b) is a result of ultrasound biomicroscopy imaging on led line in the figure (a).**

### 3.5 3-Dimensional stereoscopic imaging

Figure 18 represents a result of the SAD matching method using a stereo image through two fiber bundle. Disparity range is 16, it means maximum differential value is 16, window size is 5. In the depth map which is shown right of figure 18, A' area can be seen that the difference appears more than 10 pixel area B' area. Using formula (3), calculated surface roughness value is 0.45. It means that the surface is not strike.

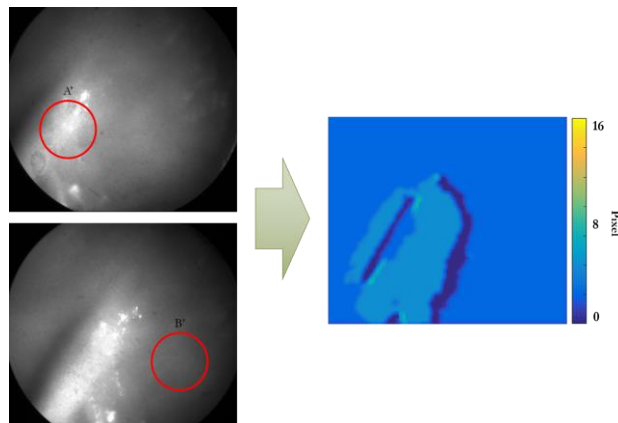


**Figure 18. 3D reconstructed image from stereo image form phantom.**

### 3.6 GPU speed experiment

In order to achieve real time image processing, we applied a GPU programming which is CUDA library. Because processing time of the SAD matching method is too long. This method depends on the disparity range and window size. Larger window size or disparity range is the processing time is longer when shift the entire image. So, an operation to copy the data to the General Purpose Graphic Processing Unit (GPGPU) was running parallel. When we set the disparity range is 16 and window size is 5, processing time represent about figure 19 according to image size. In the 888x720, difference of processing time indicates 42 times on the GPU and CPU. This result will be the larger the disparity range and window size difference is more going on.

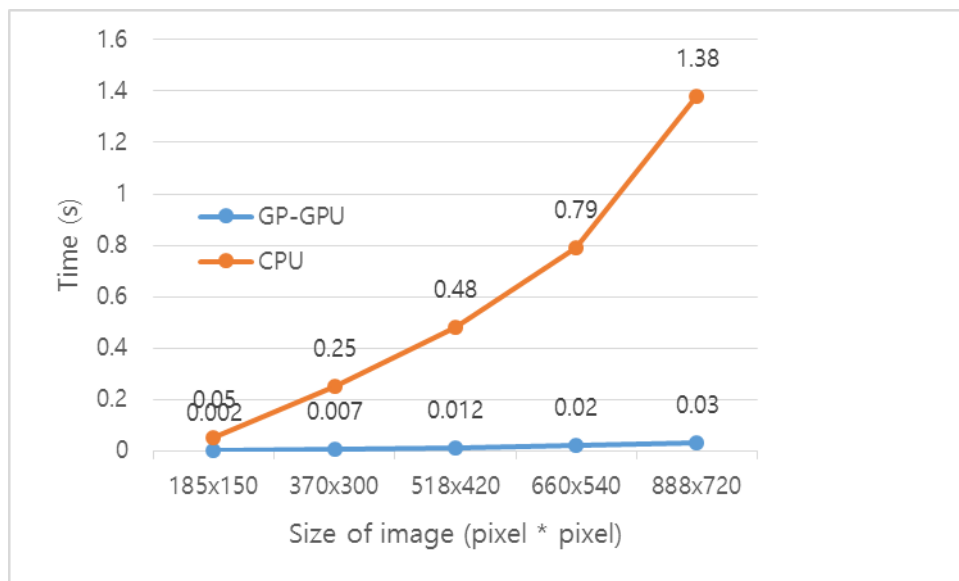


**Figure 19. comparison of the processing time of different image size**

## IV. TUMOR EXPERIMENT *ex vivo*

### 4.1 Colorectal tumor experiment ex-vivo

Using the tumor phantom figure 20(a), we performed a colorectal tumor *ex-vivo* experiment using the multimodal endoscope system. For fluorescence imaging, 488nm wavelength light is illuminated tumor area. Then, we confirmed that the strongest fluorescence appears in the tumor area. Used optical filter is 540nm bandpass filter.

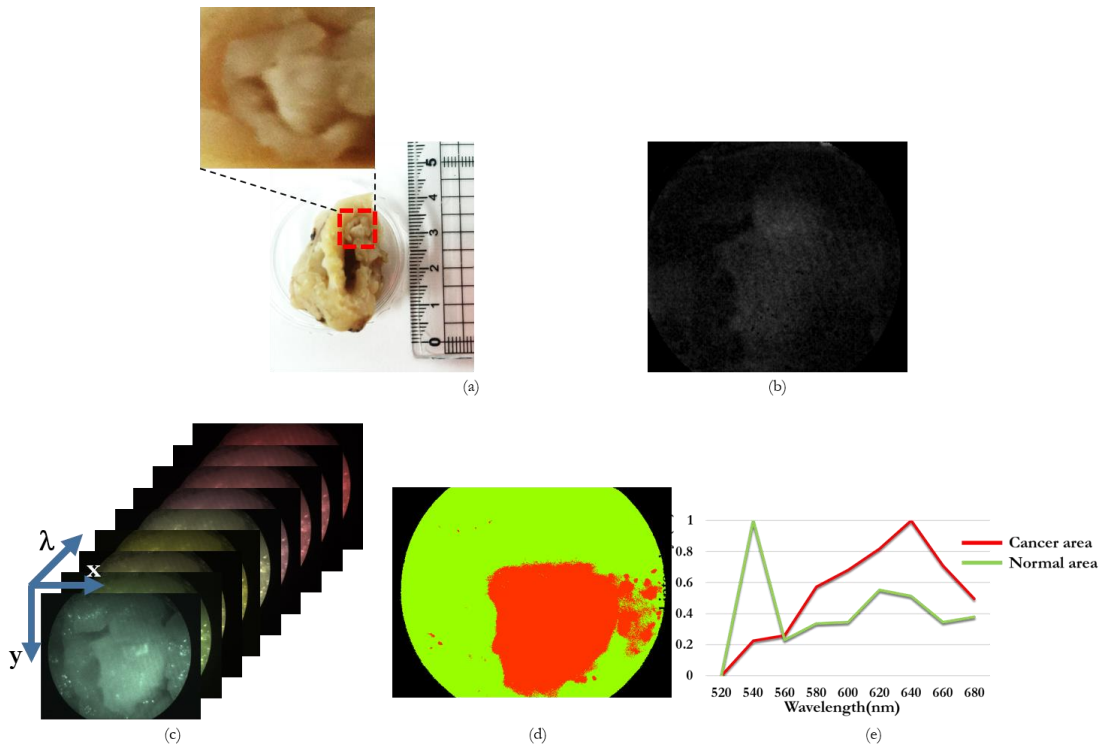
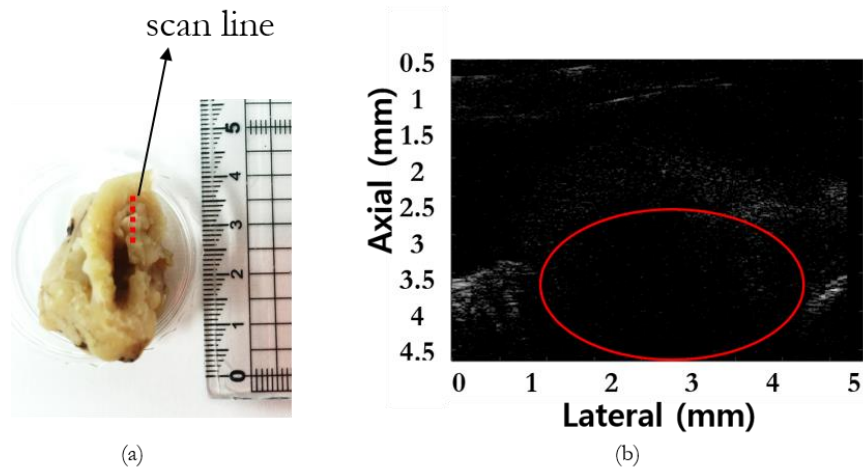


Figure 20. (a) is the colorectal tumor phantom. (b) represents about result of the fluorescence intensity imaging. Wavelength of excitation light is 488nm. Used optical filter for the fluorescent is 540nm bandpass filter. (c) represents about reflectance spectral image cube (520-680nm). (d) is a classified image from the spectral image cube (c). Red color represents tumor area. Green color represents normal and hole. Their spectral signatures are indicated as a (e).

Also, using the reflectance spectral imaging, we indicated the normal and tumor area in the same region. Used range of the optical bandpass filter is 520-680nm. And, spectral signatures of the normal and tumor is indicated as a figure 20(e). We confirmed that normal area has a peak at the 540nm and tumor area has a peak at the 640nm.



**Figure 21. (b) represents about result of the ultrasound biomicroscopy from colorectal tumor in the (a).**

At the same region, we performed the ultrasound biomicroscopy for confirmation of the invasion depth. In the figure 21(b), a red circle represents tumor area and we confirmed that invasion depth is over 2mm.

## V. DISCUSSION and CONCLUSIONS

We built a multimodal endoscope including auto-fluorescence, spectral, and real-time 3D imaging based on GPGPU programming and further incorporate it with a high-frequency ultrasound imaging unit. We performed multimodal imaging of a tissue phantom for the evaluation of the system. Here fluorescence, spectral, 3D, and high frequency ultrasound images were successfully acquired using it. In this phantom experiment, wood stick area in the pig's stomach was detected through each of an imaging mode. In particular, the real-time 3D imaging of a target region could be obtained in real-time. The acquisition time was  $\sim 0.02$  second. We thus obtained the information on surface roughness from the phantom using the real-time 3D reconstruction from stereoscopic image. However, since CCD sensor has limitations in time-lapse imaging, we will perform real-time 3D video-rate imaging after overcoming of the limitations. In the *ex-vivo* tumor experiment, colon tumors were clearly discriminated from normal regions through the reflectance spectral imaging, fluorescence imaging, and ultrasound biomicroscopy. Thus, these results demonstrate that our developed system provides multiple information on the gastric lesions of interest and therefore may allow more reliable outcomes in the early detection of colorectal lesions with high sensitivity and specificity. Furthermore, the developed system will be integrated with a high-frequency ultrasound system to obtain anatomical information below the surface of gastric lesions.

## VI. References

- [1] Martinez-Herrera, Sergio E., et al. "Multispectral Endoscopy to Identify Precancerous Lesions in Gastric Mucosa." *Image and Signal Processing*. Springer International Publishing, 2014. 43-51.
- [2] Galeano, J., Jolivot, R., Benezeth, Y., Marzani, F., Emile, J.-F., Lamarque, D.: Analysis of Multi-spectral Images of Excised Colon Tissue Samples Based on Genetic Algorithms. In: Int. Conf. on Signal Image Technology & Internet Based Systems (SITIS), Naples, Italy, November 25-29, pp. 833–838 (2012)
- [3] Kiyotoki, S., Nishikawa, J., Okamoto, T., Hamabe, K., Saito, M., Goto, A., Fujita, Y., Hamamoto, Y., Takeuchi, Y., Satori, S., Sakaida, I.: New method for detection of gastric cancer by hyperspectral imaging: A pilot study. *Journal of Biomedical Optics* 18(2), 26010 (2013)
- [4] Kobayashi, Masahiko, et al. "Detection of early gastric cancer by a real-time autofluorescence imaging system." *Cancer letters* 165.2 (2001): 155-159.
- [5] Faris, Sadeg M. "Novel 3D stereoscopic imaging technology." *IS&T/SPIE 1994 International Symposium on Electronic Imaging: Science and Technology*. International Society for Optics and Photonics, 1994.
- [6] Zhou, Lanlan, and Wafik S. El-Deiry. "Multispectral fluorescence imaging." *Journal of Nuclear Medicine* 50.10 (2009): 1563-1566.
- [7] K. Izuishi, H. Tajiri, M. Ryu, J. Furuse, Y. Maru, K. Inoue, M. Konishi, T. Kinoshita, Detection of bile duct cancer by auto-fluorescence cholangioscopy: a pilot study, *Hepato-gastroenterology* 46 (1999) 804±807.
- [8] H. Tajiri, M. Kobayashi, S. Yoshida, Fluorescence endoscopy in the gastrointestinal tract, *Dig. Endosc.* (2001) 12 in press.
- [9] Tomatis, S., Carrara, M., Bono, A.: Automated melanoma detection with a novel multispectral imaging system: Results of a prospective study. *Physics in Medicine and Biology* 50(8), 1675–1687 (2005)
- [10] Qin, A.K., Suganthan, P.N., Liang, J.J.: A new Generalized LVQ Algorithm via Harmonic to

Minimumm Distance Measure Transition, Systems. In: IEEE International Conference on Man and Cybernetics, vol. 5, pp. 4821–4825 (2004)

[11] Wong Kee Song, L. M., Adler, D. G., Conway, J. D., Diehl, D. L., Farraye, F. A., Kantsevov, S.V., Kwon, R., Mamula, P., Rodriguez, B., Shah, R. J., Tierney, W. M.: Narrow band imaging and multiband imaging. *Gastrointestinal Endoscopy* 67(4), 581-589 (2008)

[12] Zuiderveld, K.: Contrast Limited Adaptive Histogram Equalization, *Graphic Gems IV*, pp. 474–485. Academic Press Professional, San Diego (1994)

[13]. W. K. Leung, M. Wu, Y. Kakugawa, J. J. Kim, K. G. Yeoh, K. L. Goh, K. C. Wu, D. C. Wu, J. Sollano, U. Kachintorn, T. Gotoda, J. T. Lin, W. C. You, E. K. Ng, J. J. Sung, “Screening for gastric cancer in Asia: current evidence and practice” *Lancet. Oncol.* 9, 279-287 (2008).

[14]. A. J. Overhiser, P. Sharma, “Advances in endoscopic imaging: narrow band imaging” *Rev. Gastroenterol. Disord.* 8, 186 (2008).

[15]. I. Georgakoudi, B. C. Jacobson, J. Van Dam, V. Backman, M. B. Wallace, M. G. Müller, Q. Zhang, K. Badizadegan, D. Sun, G. A. Thomas, L. T. Perelman, M. S. Feld. “Fluorescence, reflectance, and lightscattering spectroscopy for evaluating dysplasia in patients with Barrett’s esophagus” *Gastroenterology* 120, 1620-1629 (2001).

[16]. Z. Huang, M. S. Bergholt, W. Zheng, K. Lin, K. Y. Ho, M. Teh, K. G. Yeoh, “In vivo early diagnosis of gastric dysplasia using narrow-band image-guided Raman endoscopy” *J. Biomed. Opt.* 15, 037017 (2010)

[17]. Z. Huang, S. K. Teh, W. Zheng, K. Lin, K. Y. Ho, M. Teh, K. G. Yeoh, “In vivo detection of epithelial neoplasia in the stomach using image-guided Raman endoscopy” *Biosens. Bioelectr.* 26, 383-389 (2010).

[18]. M. S. Bergholt, W. Zheng, K. Lin, K. Y. Ho, M. Teh, K. G. Yeoh, J. B. Y. So, Z. Huang, “In vivo diagnosis of gastric cancer using Raman endoscopy and ant colony optimization techniques” *Int. J. Cancer*, DOI: 10.1002/ijc.25618. (2010).

[19]. Park, Jae-Gahb, et al. "Characteristics of cell lines established from human gastric carcinoma." *Cancer research* 50.9 (1990): 2773-2780.

[20]. Song, Mingjun, and Tiing Leong Ang. "Early detection of early gastric cancer using image-enhanced endoscopy: Current trends." *Gastrointestinal Intervention* 3.1 (2014): 1-7.

[21]. Wang, Wenfeng, et al. "Roles of linear and circular polarization properties and effect of wave-

length choice on differentiation between ex vivo normal and cancerous gastric samples." *Journal of biomedical optics* 19.4 (2014): 046020-046020.

[22]. Shao, Xiaozhuo, Wei Zheng, and Zhiwei Huang. "Polarized near-infrared autofluorescence imaging combined with near-infrared diffuse reflectance imaging for improving colonic cancer detection." *Optics express* 18.23 (2010): 24293-24300.

[23]. Mayinger, Brigitte, et al. "Evaluation of in vivo endoscopic autofluorescence spectroscopy in gastric cancer." *Gastrointestinal endoscopy* 59.2 (2004): 191-198.

[24]. Peixinho, C. C., et al. "Ultrasound biomicroscopy for biomechanical characterization of healthy and injured triceps surae of rats." *The Journal of experimental biology* 214.22 (2011): 3880-3886.

[25]. Akbari, Hamed, et al. "Hyperspectral imaging and quantitative analysis for prostate cancer detection." *Journal of Biomedical Optics* 17.7 (2012): 0760051-07600510.

[26]. Akahoshi, K., et al. "Preoperative evaluation of gastric cancer by endoscopic ultrasound." *Gut* 32.5 (1991): 479-482.

[27]. Zeng, Haishan, et al. "Real-time endoscopic fluorescence imaging for early cancer detection in the gastrointestinal tract." *Bioimaging* 6.4 (1998): 151-165.

[28]. XIAO, Shu Dong, et al. "Diagnosis of gastric cancer by using autofluorescence spectroscopy." *Chinese Journal of Digestive Diseases* 3.3 (2002): 99-102.

[29]. Ttofis, Christos, et al. "Edge-directed hardware architecture for real-time disparity map computation." *Computers, IEEE Transactions on* 62.4 (2013): 690-704.

[30]. Bok, Tae-Hoon, et al. "Implementation of a Rotational Ultrasound Biomicroscopy System Equipped with a High-Frequency Angled Needle Transducer—Ex Vivo Ultrasound Imaging of Porcine Ocular Posterior Tissues." *Sensors* 14.9 (2014): 17807-17816.

[31]. Hwang, Jae Youn, et al. "A multimode optical imaging system for preclinical applications in vivo: technology development, multiscale imaging, and chemotherapy assessment." *Molecular Imaging and Biology* 14.4 (2012): 431-442.

[32]. Bergholt, Mads Sylvest, et al. "In vivo Raman spectroscopy integrated with multimodal endoscopic imaging for early diagnosis of gastric dysplasia." *BiOS*. International Society for Optics and Photonics, 2010.

- [33]. Bergholt, Mads Sylvest, et al. "Multimodal endoscopic imaging and Raman spectroscopy for improving in vivo diagnosis of gastric malignancies during clinical gastroscopy." *Asia Communications and Photonics Conference and Exhibition*. International Society for Optics and Photonics, 2010.
- [34]. Sun, Yinghua, et al. "Endoscopic fluorescence lifetime imaging for in vivo intraoperative diagnosis of oral carcinoma." *Microscopy and Microanalysis* 19.04 (2013): 791-798.
- [35]. Yang, Joon-Mo, et al. "Simultaneous functional photoacoustic and ultrasonic endoscopy of internal organs in vivo." *Nature Medicine* 18.8 (2012): 1297-1302.
- [36]. Yova, Dido, et al. "Development of a fluorescence-based imaging system for colon cancer diagnosis using two novel rhodamine derivatives." *Lasers in Medical Science* 15.2 (2000): 140-147.
- [37]. Zonios, George I., et al. "Fluorescence spectroscopy for colon cancer diagnosis." *Fifth International Photodynamic Association Biennial Meeting*. International Society for Optics and Photonics, 1994.
- [38]. Soletti, Rossana C., et al. "Simultaneous follow-up of mouse colon lesions by colonoscopy and endoluminal ultrasound biomicroscopy." *World journal of gastroenterology: WJG* 19.44 (2013): 8056.
- [39]. Rex, Douglas K., and Claire C. Helbig. "High yields of small and flat adenomas with high-definition colonoscopes using either white light or narrow band imaging." *Gastroenterology* 133.1 (2007): 42-47.
- [40]. Sambongi, Masao, et al. "Analysis of spectral reflectance using normalization method from endoscopic spectroscopy system." *Optical review* 9.6 (2002): 238-243.
- [41]. Park, Jinhyoung, et al. "Acoustic radiation force impulse (ARFI) imaging of zebrafish embryo by high-frequency coded excitation sequence." *Annals of biomedical engineering* 40.4 (2012): 907-915.
- [42]. Graham, Kevin C., et al. "Three-dimensional high-frequency ultrasound imaging for longitudinal evaluation of liver metastases in preclinical models." *Cancer Research* 65.12 (2005): 5231-5237.
- [43]. Sun, Lei, et al. "A high-frame rate high-frequency ultrasonic system for cardiac imaging in mice." *Ultrasonics, Ferroelectrics, and Frequency Control, IEEE Transactions on* 54.8 (2007): 1648-1655.
- [44]. Foster, F. Stuart, et al. "Advances in ultrasound biomicroscopy." *Ultrasound in medicine & bi-*

ology 26.1 (2000): 1-27.

[45]. Allen, Jason, et al. "Lower-limb vascular imaging with acoustic radiation force elastography: demonstration of in vivo feasibility." *Ultrasonics, Ferroelectrics, and Frequency Control, IEEE Transactions on* 56.5 (2009): 931-944.

[46]. Demos, S. G., and R. R. Alfano. "Optical polarization imaging." *Applied Optics* 36.1 (1997): 150-155.

[47]. Shen, Huamei, et al. "Evodiamine inhibits proliferation and induces apoptosis in gastric cancer cells." *Oncology Letters* 10.1 (2015): 367-371.

[48]. Jin, Minxi, and Tsutomu Maruyama. "A fast and high quality stereo matching algorithm on FPGA." *Field Programmable Logic and Applications (FPL), 2012 22nd International Conference on.* IEEE, 2012.

[48]. Chang, Ping-Lin, et al. "Robust real-time visual odometry for stereo endoscopy using dense quadrifocal tracking." *Information Processing in Computer-Assisted Interventions.* Springer International Publishing, 2014. 11-20.

[49]. Chung, Alice, et al. "In vivo cytometry: a spectrum of possibilities." *Cytometry Part A* 69.3 (2006): 142-146.

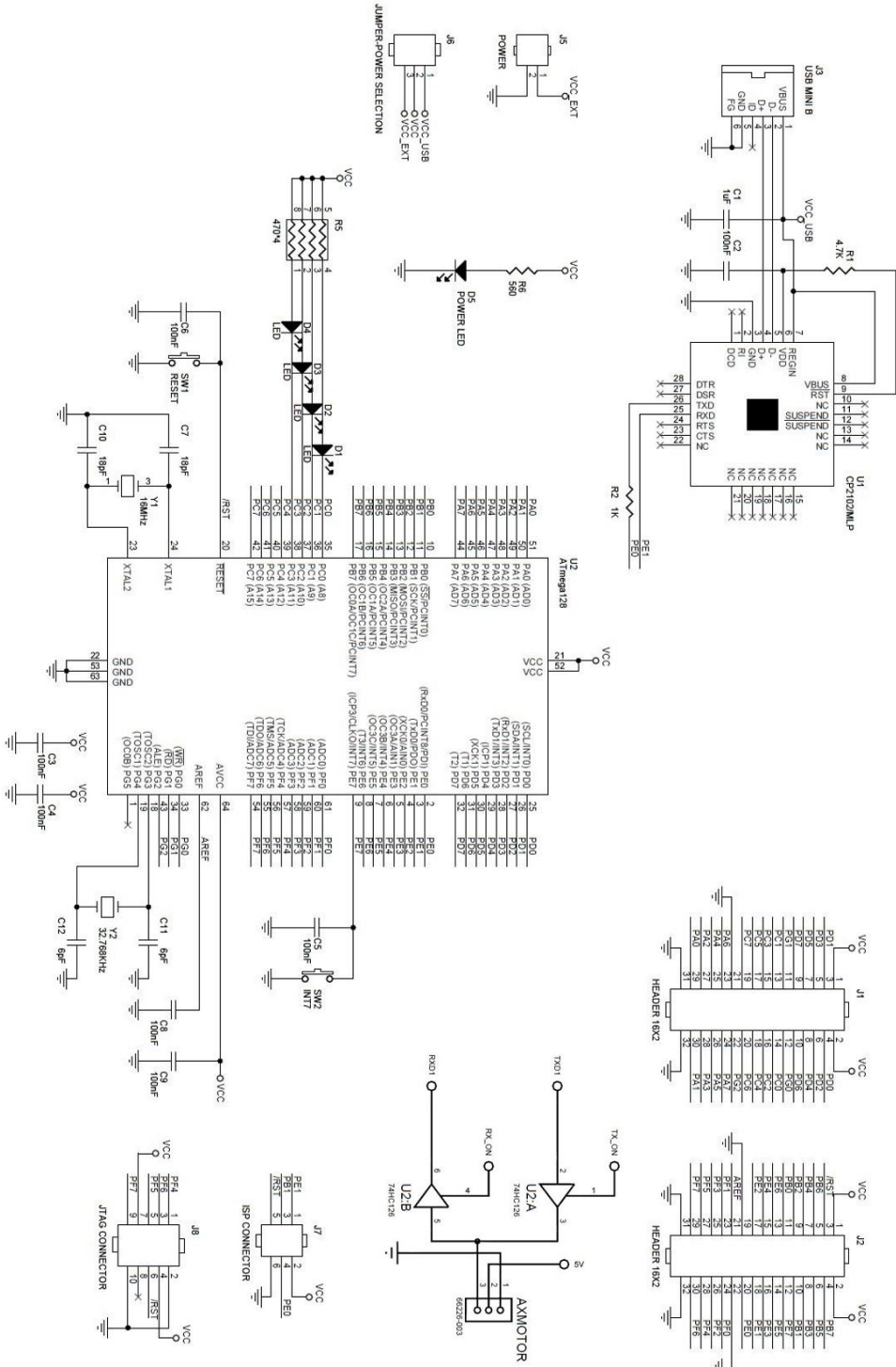
[50]. Namati, E., M. J. Suter, and G. McLennan. "Endoscopic techniques for optical imaging." *Optical Imaging of Cancer.* Springer New York, 2010. 25-48.

[51]. Spriet, Mathieu P., et al. "Validation of a 40MHz B-scan ultrasound biomicroscope for the evaluation of osteoarthritis lesions in an animal model." *Osteoarthritis and cartilage* 13.2 (2005): 171-179.

# VII. Appendix

ATmega128 board

- circuit



## 요 약 문

### 위암 검출을 위한 실시간 3차원 다중모드 내시경시스템 개발에 관한 연구

전 세계적으로, 위암은 4 번째로 많이 발생하는 악성 질병일 뿐만 아니라, 2 번째로 그 사망률이 높은 암이다. 위암이 발병한지 3 년이 지나면 환자의 생존율은 2% 이하로 떨어지지만, 6 개월 이내에 치료를 할 경우 환자의 생존율은 67% 이상으로 높아지는 것으로 알려져 있다. 그래서, 위암의 조기 진단은 그 생존율이 높이에 가장 중요한 요소 중의 하나이다. 위암을 진단하는 방법으로는 상부위장조영술(UGI), 내시경적 초음파검사, 전산화단층촬영(CT), 자기공명영상(MRI), 그리고 양전자방출단층촬영(PET) 등이 있다. 특히, 위암을 진단하는 방법으로는 내시경 방법을 가장 많이 사용하는데, 그 이유는 신체에 유해하지 않고, 비용이 적게 든다는 장점이 있기 때문이다. 그래서, 지금까지 다양한 내시경 영상을 이용한 위암 부위의 자기형광의 패턴을 분석하여 질병을 진단 하는 방법, 고주파 초음파 검사를 통해 암의 침투 정도를 분석하는 방법, 그리고 다중분광이미징을 통해 정상부위와 위암부위의 스펙트럼 특성의 차이를 분석하는 방법등 다양한 위암 검출 방법이 제시되었으나, 이러한 방법들은 그 진단의 정확도가 높지 않은 것으로 보고되어 왔다. 그래서 진단 정확도를 높이기 위해 동시에 각 이미징 특성들을 획득하는 방법들이 연구되어왔으나, 여전히 획기적인 이미징 시스템 개발이 필요한 것으로 보고되고 있다. 그래서 본 논문에서는 형광, 반사/형광 다중 분광, 실시간 3D 스테레오, 또한 초음파 이미징이 가능한 다중모드 내시경 시스템을 제안한다. 각 이미징 방식의 유효성은 돼지 위의 조직을 이용한 팬텀 이미징으로 검증을 하였다. 위 표면에 형광 염색된 나무조각을 삽입하여 실험용 팬텀을 제작하여 각 이미징 기법의 유효성을 파악 할 수 있었다. 또한, 더욱 정확한 검증을 위해 실제 대장암 모델을 사용하여 정상부위와 암부위의 이미징을 통해 암 영역과 정상영역을 구분하는 실험을 시행하였고, 그 결과 각각의 이미징 기법에서 암영역과 정상영역을 구분 할 수 있다는 것을 확인하였다. 이 결과로부터 개발된 시스템은 위 병변의 조기진단에 있어서의 자기형광의 강도, 분광지표 및 3 차원 표면 곡률과 같이 위의 병변에서 서로 다르지만 상호보완적인 정보를 얻을 수 있어, 진단하는데 있어서 그 정확도를 높일 수 있는 그 가능성을 보여주었다.

핵심어: 멀티모달 이미징, 자기 형광, 다중 분광, 3차원 이미징, 고주파 초음파 이미징